journal

J. Am. Ceram. Soc., **82** [3] 616–24 (1999)

Elastic and Yield Behavior of Strongly Flocculated Colloids

Wan Y. Shih,[†,‡] Wei-Heng Shih,[*,‡] and Ilhan A. Aksay[*,†]

Department of Chemical Engineering and Princeton Materials Institute, Princeton University, Princeton, New Jersey 08544-5263; and
Department of Materials Engineering, Drexel University, Philadelphia, Pennsylvania 19104-2875

We have investigated theorectically the elastic and yield behaviors of strongly flocculated colloids by first examining the yield forces between two particles within the framework of Derjaguin–Landau–Verwey–Overbeck (DLVO) interactions. Under highly attractive conditions, i.e., in the absence of the secondary minimum in the DLVO potential, the radial (tensile) motion between particles is nonelastic because of the lack of an inflection point in the DLVO potential. However, the lateral (shear) motion is shown to be elastic up to a distance y_{max}, providing a mechanism for the observed elasticity in colloidal gels. If r_0 and s_0 are, respectively, the closest center-to-center and surface-to-surface distances between two particles,

$$y_{max} \propto (1 - 0.5\alpha\zeta^2)(s_0 r_0)^{1/2}$$

where ζ is the zeta potential of the particles and α a defined constant. Moreover, the yield force between two particles is much smaller in the lateral direction than in the radial direction. These results suggest that yielding of a particulate network is likely to occur through the lateral movements between particles. The yield strain can be approximated as that at which all the bonds in a certain direction have a perpendicular displacement $>y_{max}$, resulting in

$$\epsilon_{yield} = \frac{y_{max}}{r_0} \propto (1 - 0.5\alpha\zeta^2)\left(\frac{s_0}{r_0}\right)^{1/2}$$

The shear modulus of the network, G', can be deduced by combining the elastic constant of the lateral movement with the existing elastic theory of a particulate network. The yield stress can be approximated as

$$\sigma_{yield} \approx G'\epsilon_{yield} \propto (1 - 1.5\alpha\zeta^2)\frac{A}{24 s_0^{3/2}}\frac{1}{R^{d-3/2}}$$

where A is the Hamaker constant and R the particle radius. These predictions are shown to compare favorably with existing experiments.

I. Introduction

One of the potential benefits of colloidal processing is its utility in fabrication of complex-shaped ceramics.[1–9] Because of their high rigidity at low shear, flocculated suspensions have become more important for forming and shaping.[9–14] High rigidity often translates to poor flowability under shear,[4,5] and high flowability at high shear rate often is accompanied by creep.[4,5] To circumvent these problems, current technology uses polymers as gelling agent to provide proper rheological properties for forming.[6–8] Using polymers as forming aids, however, has the disadvantage of decreased packing densities[6–8] and problems associated with polymer burnout. Recent experiments on suspensions of boehmite-coated silicon nitride have revealed that such suspensions have a remarkable capability for green-state deformation,[3,4] suggesting the possibility of forming ceramics without the use of polymers as done in clay-based systems.

If forming and shaping are to be successful, the suspension must possess proper ridigity (solidlike) at low shear rates and reasonable flowability (liquidlike) at high shear rates. Experiments have shown that the suspension rheology can be manipulated by varying the short-range interparticle forces,[3–5,9–12,15,16] the pH,[15,16] the zeta potential,[16,17] and the particle size.[11,15–19] However, a thorough understanding of the solidlike-to-liquidlike transition upon shear remains lacking. It is essential to understand the solid-to-liquid transition under shear to explore the feasibility of forming and shaping ceramics without excessive use of polymers.

Many experiments have examined such transitions by measuring the shear yield stress[11,15–22] or the compressive yield stress.[12,18,20] Both stresses have been shown to increase as a power law of particle concentration with an exponent identical to that of the storage modulus.[20] Another way to characterize the yield behavior of a suspension is to do constant-strain measurements with a dynamic rheometer.[23–27] With respect to the strain amplitude ϵ, the storage modulus G' and the loss modulus G'' are measured, where G' is proportional to the shear modulus of the particulate network and G'' proportional to the suspension viscosity. If the concentration is high enough, a flocculated suspension may exhibit as many as three distinctive regimes in such measurements, as schematically shown in Fig. 1. At low ϵ, the solid regime occurs, (regime I), where G' is more-or-less constant with respect to ϵ and $G' > G''$. At intermediate ϵ, the solid-to-liquid transition occurs (regime II), where G' decreases sharply while G'' undergoes a maximum.

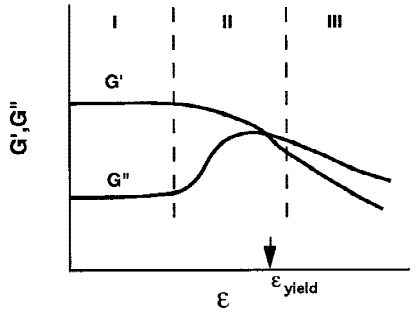

Fig. 1. Schematic of the storage modulus, G', and loss modulus, G'', versus the strain amplitude, ϵ, for a flocullated suspension measured by a rheometer. Region I is the solid regime where $G' > G''$. Region II is the solid–liquid transition region where G' decreases sharply and G'' undergoes a maximum. Region III is the liquid region where $G' < G''$.

C. F. Zukoski—contributing editor

Manuscript No. 191220. Received February 7, 1997; approved May 12, 1998.
*Member, American Ceramic Society.
†Princeton University.
‡Drexel University.

At high ϵ, the liquid regime occurs (regime III), where $G'' > G'$. The yield strain, ϵ_{yield}, is defined as the strain amplitude at which G' and G'' cross and the yield stress is $\sigma_{yield} \propto G'\epsilon_{yield}$. Quantitatively, σ_{yield} may be somewhat different from the shear yield stress measured in the constant-stress mode or the compressive yield stress obtained in consolidation experiments. Moreoever, ϵ_{yield} exhibits a marked dependence on particle size. Suspensions of smaller particles usually exhibit a larger ϵ_{yield} than suspensions of larger particles. For example, ϵ_{yield} of small boehmite[23,24,28] and silica[24] particles of ~10 nm in size is ~10%, whereas the ϵ_{yield} of alumina particles of ~400 nm in size is <1%.[28] Figures 2 and 3 show measured G' and G'' versus ϵ for a boehmite gel of 4.5 vol% (10 nm in size) at pH 3.5 with 0.244*M* KCl (from Ref. 23) and for an alumina suspension of 35 vol% (400 nm in size) at pH 8.5 (from Ref. 28), respectively. The boehmite gel exhibits a sizable solid regime with the solid-to-liquid transition occurring at $\epsilon_{yield} \approx 13\%$. In contrast, the alumina suspension exhibits a much smaller solid regime with $\epsilon_{yield} \approx 0.5\%$. Besides its particle-size dependence, suspension ϵ_{yield} also depends on the adsorbed-layer thickness when there is an adsorbed layer on the particle surface. For example, when the alumina particles are adsorbed with a surfactant layer, ϵ_{yield} can be increased to as high as 20%.[29] Polystyrene spheres known to have an adsorbed layer on the particle surface and polystyrene spheres of ~200 nm in size also can exhibit a sizable solid regime with $\epsilon_{yield} \approx 10\%$.[18,30] The existing models explain the yielding in terms of radial movements between particles.[31–33] If a short-range repulsion energy[33] or an electrostatic repulsion energy is considered,[31,32] ϵ_{yield} is estimated using the inflection point of the interparticle interaction energy in the radial direction[31,32] or using a characteristic distance beyond which the interaction energy is larger than a certain value.[33] ϵ_{yield} values obtained by such analyses are typically <1%,[18,33] unable to explain the large ϵ_{yield} value observed in the boehmite,[23,24,28] silica,[24] polystyrene,[18,30] and coated-alumina[29] systems.

The concentration dependence of G' in the solid regime has been studied extensively.[18,20–30,34] G' has been shown to increase as a power law of concentration in the absence of extensive particulate restructuring.[18,20–26] When the particulate network is treated as a spring network, the power-law dependence of G' directly results from the fractal structure of the clusters that pack to form the network.[23] These results are useful in that they help establish the correlation between the rheological properties and the structure of an aggregated network. Although much progress has been made in understanding the structural dependence of the elastic property in the solid regime, the mechanism for the elastic response has been largely overlooked. The yielding of a network is basically a transition from an elastic solid state to a liquid state. That the existing

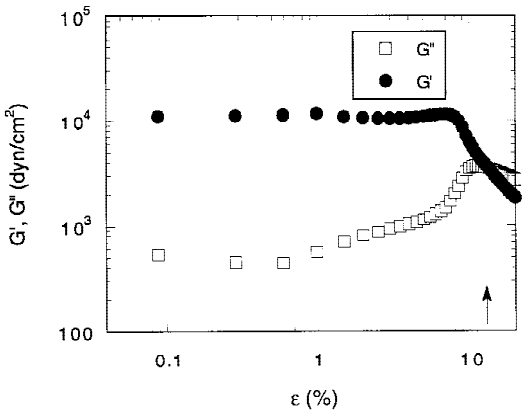

Fig. 2. Storage modulus, G', and loss modulus, G'', versus the strain amplitude, ϵ, of a 4.5 vol% boehmite gel with 0.244*M* KCl, redrawn from Ref. 23. Arrow marks the yield strain, ~13%, as defined in the text. Size of the boehmite particles is ~10 nm.[23]

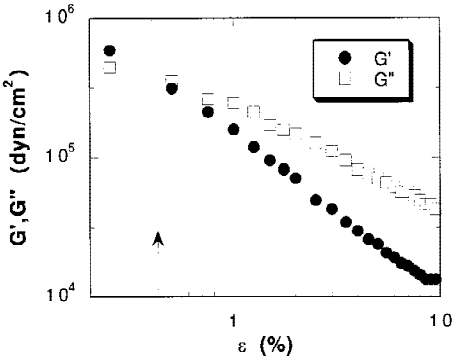

Fig. 3. Storage modulus, G', and loss modulus, G'', versus the strain amplitude, ϵ, for a flocculated alumina suspension of 35 vol% at pH 8.5, redrawn from Ref. 28. Yield strain, as marked by the arrow, is <0.5%, much smaller than that of the boehmite gel.

yield models[31–33] cannot explain the large yield strains observed in the boehmite,[23,24,28] silica,[24] polystyrene,[18,30] and coated-alumina[29] systems by considering radial movements indicates that other types of movements also should be examined. In this paper, we theoretically investigate the elastic and yield behaviors of strongly aggregated particulate networks by considering lateral movements within the framework of the Derjaquin-Landau-Verwey-Overbeek (DLVO) interactions.

II. Theory

(1) Interparticle Forces

The interparticle DLVO interaction energy can be written as[35]

$$V(s) = V_R(s) + U(s) \tag{1}$$

where $V_R(s)$ and $U(s)$ are the interparticle repulsion energy and attraction energy, respectively, and s the surface-to-surface distance along the center-to-center line between the particles. $U(s)$ can be approximated as

$$U(s) = -\frac{A}{6}\left[\frac{2R^2}{s^2+4Rs} + \frac{2R^2}{s^2+4Rs+4R^2} + \ln\left(\frac{s^2+4Rs}{s^2+4Rs+4R^2}\right)\right] \tag{2}$$

where R is the radius of the particles and A the Hamaker constant. The Hamaker constant with water as the medium can be calculated using the Tabor–Winterton approximation:[36]

$$A = \frac{3}{4}k_BT\left(\frac{\varepsilon-\varepsilon_w}{\varepsilon+\varepsilon_w}\right)^2 + \frac{3}{16}\frac{h\omega}{2^{1/2}}\frac{(n^2-n_w^2)^2}{(n^2+n_w^2)^{3/2}} \tag{3}$$

where ε and ε_w are the static dielectric constants of the particles and water, respectively, n and n_w the indexes of refraction of the particles and water, respectively, and ω the relaxation frequency of the dielectric function. For $s << R$, $V_R(s)$ at constant potentials can be approximate as[37]

$$V_R(s) = 2\pi\varepsilon_0\varepsilon_w R\zeta^2 \ln(1+e^{-\kappa s}) \tag{4}$$

where ζ is the zeta potential of the particles, $\varepsilon_0 = 8.85 \times 10^{-12}$ $C^2 \cdot J^{-1} \cdot m^{-1}$, κ the inverse of the screening length in the Debye–Hückel approximation; i.e.,

$$\kappa^2 = (e^2/\varepsilon_0\varepsilon_w k_BT)\Sigma n_i z_i^2 \tag{5}$$

where k_B is the Boltzmann constant, T the temperature, and n_i and z_i the number density and charge of the ith species ions in the solution.

Strong aggregation occurs when the electrostatic repulsion

between particles is absent or much reduced. This can happen when a nonpolar solvent is used or when the pH of an aqueous suspension is near the isoelectric point (IEP) and/or when a large amount of electrolyte is added to the aqueous suspension. Under such conditions, the interparticle interaction is dominated by the van der Waals attraction. As an example, we show the DLVO $V(s)$ versus s in Figs. 4 and 5 for alumina particles of 10 and 200 nm in size, respectively. $V_R(s)$ has been calculated using Eq. (4). The electrolyte concentration has been taken as 0.25*M*, which corresponds to $\kappa = 1.6 \times 10^9\ m^{-1}$. Also, $A = 4.5 \times 10^{-20}$ J for alumina has been obtained using Eq. (3) with $\omega = 2 \times 10^{16}$ rad/s, and values of ε and n taken from Ref. 38. At such a high electrolyte concentration, the DLVO interaction is mainly attractive, and only the primary minimum is present. All of the DLVO curves in Figs. 4 and 5 show no inflection points. The lack of an inflection point in the DLVO $V(s)$ is related to the absence of a secondary minimum and can be understood as follows. For $s << 2R$, the leading term in the van der Waals attraction energy has the following form:

$$U(s) \approx -\frac{AR}{12s} \tag{6}$$

Therefore, $U(s)$ approaches $1/s$ as s approaches zero. On the other hand, $V_R(s)$, as depicted in Eq. (4), approaches a constant when s approaches zero. Hence, the slope $dU(s)/ds$ becomes steeper as s approaches 0, resulting in no inflection point near the primary minimum at $s = 0$. Because there is no inflection point near the primary minimum, when the secondary minimum is absent, the DLVO $V(s)$ simply has no inflection point. The secondary minimum in a strongly flocculated suspension is absent in the DLVO $V(s)$. Thus, the observed elastic behavior in flocculated suspensions cannot be attributed simply to the radial movements between particles. We consider below the lateral movements between particles to explain the elastic behavior of strongly aggregated networks. As we have argued above, the present consideration is particularly important when the DLVO $V(s)$ has no secondary minimum.

(a) $\zeta = 0$: Let us first consider the case where $\zeta = 0$. We use Eq. (6) as the form of the attraction energy for the ease of discussion. As shown numerically below, this approximation is quite adequate for the present considerations where we are mainly dealing with small separations. Meanwhile, many experiments have revealed that an adsorption layer of ions or water can occur on the surface of particles[10,11,15,16,39] in aqueous suspensions. The closest surface-to-surface distance, s_0, may be finite because of the adsorption layer around the particles. Let $r = s + 2R$ be the center-to-center distance between two particles. Similarly, let $r_0 = s_0 + 2R$ be the closest center-to-center distance between two particles. A finite s_0 is important in that it weakens the bonds (or the spring constant) between particles so that particle rearrangement can occur more easily under shear. Let the initial center-to-center line between the pair be in the x direction, as depicted in Fig. 6(a). The attractive force between two particles in the x direction is

$$F_x^0 = -\frac{\partial U(s)}{\partial s}\frac{ds}{dx} \approx -\frac{AR}{12s^2} \tag{7}$$

where the 0 superscript in F_x denotes that $\zeta = 0$. At $\zeta = 0$, the DLVO $V(s)$ has no inflection point in the radial direction. F_x^0 is maximized at s_0, i.e.,

$$F_{x,\max}^0 \approx -\frac{AR}{12s_0^2} \tag{8}$$

As an example, $-F_x^0$ versus s for alumina particles of 200 nm in radius is shown in Fig. 7(a). As $-F_x^0$ decreases with increasing s, no finite *static* radial displacement can be generated with a static radial applied force, that is, no elasticity. When the static radial applied force is $< |F_{x,\max}^0|$, the displacement is simply zero. When the static radial applied force is $> |F_{x,\max}^0|$, the

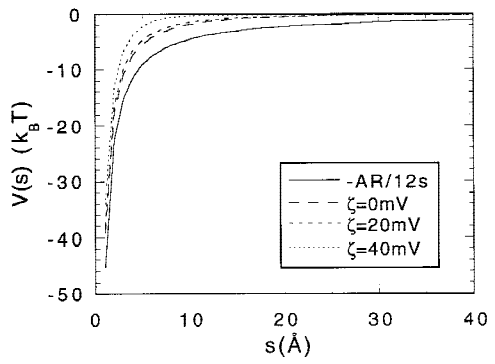

Fig. 4. DLVO interaction energy for alumina particles of $R = 10$ nm at various ζ with an electrolyte concentration of 0.25*M*. Note that all the curves lack an inflection point.

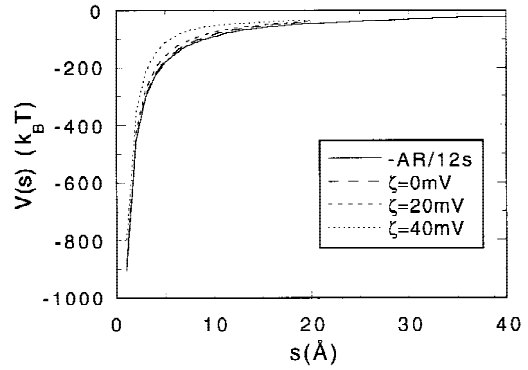

Fig. 5. DLVO interaction energy for alumina particles of $R = 200$ nm at various ζ with an electrolyte concentration of 0.25*M*. Note that all the curves lack an inflection point.

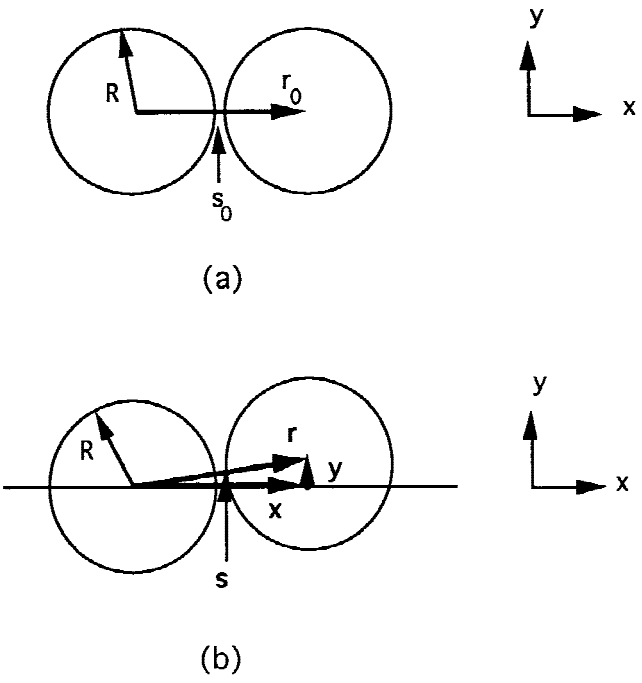

Fig. 6. (a) Schematic of the coordinates of a two-particle system with r_0 and s_0 denoting the center-to-center and surface-to-surface distances, respectively. (b) Schematic of the coordinates after the particle to the right moves in the y direction a distance y. New center-to-center and surface-to-surface distances become r and s, respectively.

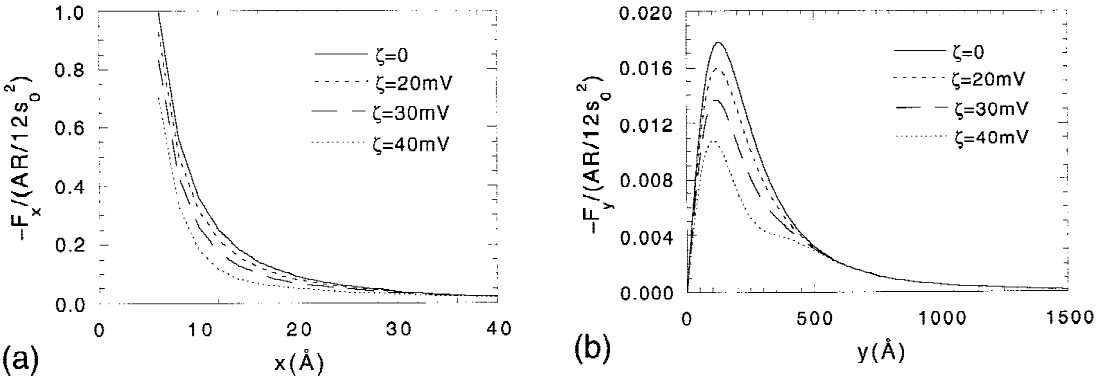

Fig. 7. (a) $-F_x$ versus x where F_x is the restoring force in the radial direction between two particles with various ζ. (b) $-F_y$ versus y where F_y is the restoring force in the lateral direction y between two particles with various ζ. Both F_x and F_y were obtained numerically from the full DLVO interaction energy using Eq. (2) as the form of attraction energy for alumina particles of $R = 200$ nm and $s_0 = 0.6$ nm with $\kappa = 1.4 \times 10^9$ m^{-1}. Note that $-F_x$ decreases monotonically as x increases, whereas $-F_y$ exhibits a maximum at an intermediate $y = y_{max}$. Note that y_{max} decreases as ζ increases.

two particles continue to move away from each other, because the restoring force at any $x > s_0$ is smaller than the applied force; i.e., the displacement is not *static*, but increases with time. The lack of elasticity in the radial direction is related to the lack of an inflection point in the DLVO interaction energies under attractive conditions, as illustrated in Figs. 4 and 5. This makes the DLVO interactions different from atomic interactions, such as the Lennard–Jones potential.[40] The existence of an inflection point in the atomic interactions permits tensile elasticity in ordinary solids.

Although the yield behavior of a particulate network often is explained as a result of overcoming the radial force depicted in Eq. (8),[15,16] the radial movement alone cannot explain the elastic behavior exhibited by suspensions of small boehmite, small silica, polystyrene, and coated-alumina particles. The lack of elasticity in the DLVO $V(s)$ in the radial direction under strongly attractive conditions, i.e., in the absence of a secondary minimum in the DLVO potential, suggests that lateral forces may be important for elastic and yield behaviors of strongly flocculated suspensions.

Alternatively, if we consider the sliding of one particle relative to another in the lateral, y, direction, as schematically shown in Fig. 6(b), the attractive force is

$$F_y^0 = -\frac{\partial U(s)}{\partial s}\frac{\mathrm{d}s}{\mathrm{d}y} \approx -\frac{AR}{12s^2}\frac{y}{(r_0^2+y^2)^{1/2}} \tag{9}$$

where the 0 superscript in F_y denotes that $\zeta = 0$. Comparing Eqs. (7) and (9), $|F_y^0| < |F_x^0|$ by a factor of $y/(r_0^2 + y^2)^{1/2}$. At small y, Eq. (9) is reduced to

$$F_y^0 \approx -\frac{\partial U(s)}{\partial s}\frac{1}{r_0}y \approx -\frac{AR}{12s^2}\frac{y}{r_0} \tag{10}$$

Clearly, $-F_y^0$ increases with increasing y at small y, indicating that the sliding of one particle relative to another in the y direction is elastic at small y. The elastic constant K for y displacements is, therefore,

$$K_0 \approx \frac{\partial U(s)}{\partial s}\frac{1}{r_0} \approx \frac{A}{24s_0^2} \tag{11}$$

where the 0 subscript in K denotes that $\zeta = 0$. Because there is no elasticity in the radial direction at $\zeta = 0$, the elastic behavior of a particulate network is mainly the result of the elastic response in the lateral direction. Moreover, F_y^0 can be rewritten as

$$F_y^0 \approx -\frac{AR}{12s_0^2 r_0}\frac{y}{[1+y^2/(2r_0 s_0)]^2} \tag{12}$$

The term $y/[1 + y^2/(2r_0 s_0)]^2$ has a maximum at

$$y_{max}^0 = \left(\frac{2}{3}\right)^{1/2}(r_0 s_0)^{1/2} \tag{13}$$

where the 0 superscript in y_{max} denotes that $\zeta = 0$. Therefore, $-F_y^0$ has a maximum at y_{max}^0, as shown in Fig. 7(b)), and

$$F_{y,max}^0 \approx -\frac{AR}{12s_0^2}\frac{9}{16}\frac{y_{max}^0}{r_0} \approx -\frac{9}{16}\frac{y_{max}^0}{r_0} \approx -\frac{9}{16}K_0 y_{max}^0 \tag{14}$$

Equation (13) is derived using Eq. (6) as the form of the attraction energy, and it is quite accurate in predicting y_{max}^0. For $R = 200$ nm and $s_0 = 0.6$ nm, Eq. (13) gives $y_{max}^0 = 12.6$ nm, which agrees extremely well with what is shown in Fig. 7(b), which has been obtained numerically using Eq. (2) as the form of attraction energy. The reason is that the present analysis mainly deals with small separations where the attraction energy can be adequately represented by Eq. (6). For an applied lateral force less than $-F_{y,max}^0$, a *static* lateral displacement can be generated, and particles retract to the original separation once the force is released. If the force is larger than $-F_{y,max}^0$, however, particles continue to move away from each other, resulting in yielding. Comparing Eqs. (8) and (14), the ratio $F_{y,max}^0/F_{x,max}^0$ is

$$\frac{F_{y,max}^0}{F_{x,max}^0} = \frac{9}{16}\frac{y_{max}^0}{r_0} = \frac{9}{16}\left(\frac{2}{3}\right)^{1/2}\left(\frac{s_0}{r_0}\right)^{1/2} \tag{15}$$

Because $s_0 << r_0$, $-F_{y,max}^0 << -F_{x,max}^0$. It is much easier to break up two particles by applying a lateral force than by applying a radial force. Because of its capability for elastic response and its reduced yield force, the lateral movement, rather than the tensile movement, is responsible for network rearrangement.

(b) $\zeta \neq 0$: For $\zeta \neq 0$, the restoring force in the radial direction, F_x, becomes

$$F_x(\zeta) = -\frac{\partial U(s)}{\partial s}\frac{\mathrm{d}s}{\mathrm{d}x} \approx -\frac{AR}{12s^2} + 2\pi\varepsilon_0\varepsilon_w R\zeta^2\frac{\kappa e^{-ks}}{1+e^{-ks}} \tag{16}$$

Figure 7(a) shows that, with $\zeta \neq 0$, there continues to be no inflection point in the radial direction when the DLVO $V(s)$ has no secondary minimum and $|-F_x|$ continues to decrease monotonically. With α defined as

$$\alpha \equiv \left(2\pi\varepsilon_0\varepsilon_w\kappa\frac{e^{-ks_0}}{1+e^{-ks_0}}\right) \Big/ \left(\frac{A}{12s_0^2}\right) \tag{17}$$

the maximum of the radial restoring force at s_0, can be expressed as

$$F_{x,\max}(\zeta) = -\frac{AR}{12s_0^2}(1-\alpha\zeta^2) = F^0_{x,\max}(1-\alpha\zeta^2) \tag{18}$$

The restoring force, F_y, in the lateral direction, y, becomes

$$F_y(\zeta) = -\frac{\partial U(s)}{\partial s}\frac{\mathrm{d}s}{\mathrm{d}y} \approx \left(-\frac{AR}{12s^2} + 2\pi\varepsilon_0\varepsilon_w R\zeta^2\frac{\kappa e^{-ks}}{1+e^{-ks}}\right)\frac{y}{r_0} \tag{19}$$

Again, at small y, the lateral movements are elastic, and the lateral restoring force is lower than that of the radial direction by a factor y/r_0. The elastic constant at small y can be written as

$$K(\zeta) = \frac{A}{24s_0^2}(1-\alpha\zeta^2) = K_0(1-\alpha\zeta^2) \tag{20}$$

and the restoring force in the y direction as

$$F_y(\zeta) \approx \frac{A}{24s_0^2}(1-\alpha\zeta^2)\frac{y}{[1+y^2/2(1-\alpha\zeta^2)r_0s_0]^2} \tag{21}$$

The maximum restoring force, $F_{y,\max}(\zeta)$, occurs at

$$y_{\max}(\zeta) = \left(\frac{2}{3}\right)^{1/2}(1-\alpha\zeta^2)^{1/2}(s_0r_0)^{1/2} \tag{22}$$

$F_{y,\max}(\zeta)$ can be expressed as

$$\begin{aligned} F_{y,\max}(\zeta) &\approx -\frac{9}{16}K(\zeta)y_{\max}(\zeta) \\ &\approx -\frac{9}{16}\frac{A}{24s_0^2}(1-\alpha\zeta^2)^{3/2}\left(\frac{2}{3}\right)^{1/2}(r_0s_0)^{1/2} \end{aligned} \tag{23}$$

For small, $\alpha\zeta^2$,

$$y_{\max}(\zeta) \approx y^0_{\max}\left(1-\frac{1}{2}\alpha\zeta^2\right) \tag{24}$$

$$F_{y,\max}(\zeta) \approx F^0_{y,\max}\left(1-\frac{3}{2}\alpha\zeta^2\right) \tag{25}$$

and the ratio

$$\frac{F_{y,\max}(\zeta)}{F_{x,\max}(\zeta)} = \frac{9}{16}\left(\frac{2}{3}\right)^{1/2}\left(1-\frac{1}{2}\alpha\zeta^2\right)\left(\frac{s_0}{r_0}\right)^{1/2} \tag{26}$$

Equation (24) predicts that $y_{\max}$ decreases linearly with ζ^2. To determine how reliable the approximation is, we have plotted the $y_{\max}$ obtained numerically using the complete DLVO potential versus ζ^2 in Fig. 8. Indeed, $y_{\max}(\zeta)$ decreases linearly with ζ^2, indicating that Eq. (24) is a good approximation for $y_{\max}(\zeta)$. We also have plotted the numerically obtained $-F_{y,\max}(\zeta)$ versus ζ^2 in Fig. 9. Indeed, $-F_{y,\max}(\zeta)$ also decreases linearly with ζ^2

(2) Yield Strain and Yield Stress

Given the individual spring constant, the viscoelastic properties of a spring network can be related to the individual spring constant K if the structure of the network is known. When the network is formed by fractal clusters, the modulus of the network can be related to K, the particle volume fraction ϕ, and the particle radius R as[23]

$$K_{\text{net}} \propto K\frac{1}{R^{d-2}}\phi^m \tag{27}$$

where $m = (d + X)/(d - D)$ with d as the Euclidean dimension and D and X the fractal dimensions of the clusters and the backbone of the clusters, respectively.[23] Similar scaling expressions also have been obtained by Brown[41] and de Rooij *et al.*[33] Experimentally, the exponent m ranges from 3 to 5, depending on the suspension conditions.[18,21,23,24] Under most gelation conditions, $X \approx 1$.[23] Thus, an exponent of $m = 3$, 4, or 5, corresponds to a fractal dimension of $D = 1.7$, 2.0, or 2.2, respectively, which agrees with the results obtained from light-scattering experiments. With the two-particle elastic constants for lateral motion depicted in Eqs. (11) and (20) as the individual spring constants, G' of the whole network can be obtained by combining Eqs. (11), (20), and (27). For, $\zeta \neq 0$

$$G'(\zeta) \approx \frac{A}{24s_0^2}(1-\alpha\zeta^2)\frac{1}{R^{d-2}}\phi^m \tag{28}$$

For $\zeta = 0$, the storage modulus reduces to

$$G'_0 \approx \left(\frac{A}{24s_0^2}\right)\frac{1}{R^{d-2}}\phi^m \tag{29}$$

where the 0 subscript denotes $\zeta = 0$ and

$$G'(\zeta) = G'_0(1-\alpha\zeta^2) \tag{30}$$

The yielding or the solid-to-liquid transition of the network involves extensive breakdown of the network. The solid-to-liquid transition corresponds to a state when the particle pairs, with their center-to-center lines lying in the x direction, displace a distance equal to $y_{\max}$ in the y direction. This is a justifiable approximation under shear conditions for moderate to higher concentrations. The breakdown of bonds in a certain direction under shear conditions has been shown in the experiment of Ackerson and Clark,[42] where three-dimensional col-

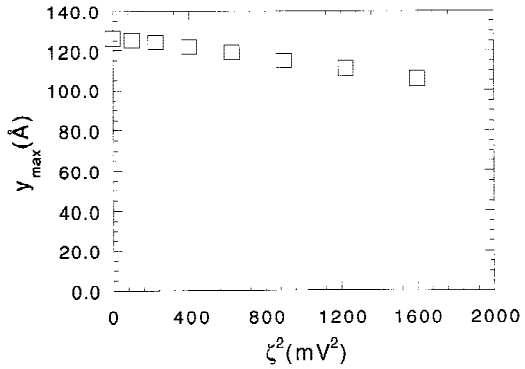

Fig. 8. $y_{\max}(\zeta)$ versus ζ^2 for the alumina particles of $R = 200$ nm and $s_0 = 0.6$ m with $\kappa = 1.4 \times 10^9$ m^{-1}·$y_{\max}(\zeta)$ is where $-F_y$ exhibits a maximum, as shown in Fig. 7(b), and was obtained numerically from the full DLVO interaction energy with Eq. (2) as the form of attraction energy. $y_{\max}(\zeta)$ decreases linearly with ζ^2, as predicted by Eq. (24). Meanwhile, $y_{\max}(\zeta = 0)$ also agrees very well with Eq. (13).

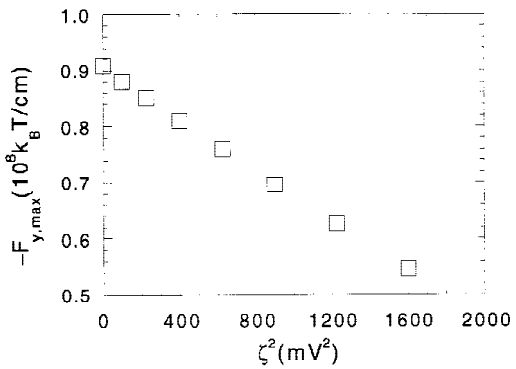

Fig. 9. $-F_{y,\max}(\zeta)$ versus ζ^2 for the alumina particles of $R = 200$ nm and $s_0 = 0.6$ nm with $\kappa = 1.4 \times 10^9$ m^{-1}. $-F_{y,\max}(\zeta)$ is the maximum in $-F_y$ as shown in Fig. 7(b) and was obtained numerically from the full DLVO interaction energy with Eq. (2) as the form of attraction energy. Note that $-F_{y,\max}(\zeta)$ decreases linearly with ζ^2, as predicted by Eq. (25) and that $-F_{y,\max}(\zeta = 0)$ agrees very well with Eq. (23).

loidal crystals have been observed to break down to layers of two-dimensional crystals at the onset of the solid-to-liquid transition under shear. Within this approximation, once the y displacement is $>y_{max}$, the particle pairs break apart, and the particles can slide relatively to each other in the y direction. The yield strain of the network can be approximated as the ratio y_{max}/r_0. Because $y_{max} << r$, the yield strain can be approximated as

$$\epsilon_{yield}(\zeta) \approx \frac{y_{max}(\zeta)}{r_0} \approx \left(\frac{2}{3}\right)^{1/2}\left(1-\frac{1}{2}\alpha\zeta^2\right)\left(\frac{s_0}{r_0}\right)^{1/2} \tag{31}$$

and, for $\zeta = 0$,

$$\epsilon^0_{yield} \approx \frac{y^0_{max}}{r_0} \approx \left(\frac{2}{3}\right)^{1/2}\left(\frac{s_0}{r_0}\right)^{1/2} \tag{32}$$

where the 0 superscript denotes that $\zeta = 0$, and,

$$\epsilon_{yield}(\zeta) = \epsilon^0_{yield}\left(1-\frac{1}{2}\alpha\zeta^2\right) \tag{33}$$

The yield stress of the network can be approximated as

$$\sigma_{yield}(\zeta) \approx G'(\zeta)\epsilon_{yield}(\zeta) \tag{34}$$

Thus, the suspension yield stress can be expressed as

$$\sigma_{yield}(\zeta) \propto \left(1-\frac{3}{2}\alpha\zeta^2\right)\frac{A}{24s_0^{3/2}}\frac{1}{R^{d-3/2}}\phi^m \tag{35}$$

For $\zeta = 0$, the suspension yield stress reduces to

$$\sigma^0_{yield} \propto \frac{A}{s_0^{3/2}}\frac{1}{R^{d-3/2}}\phi^m \tag{36}$$

where the 0 superscript in σ_{yield} denotes that $\zeta = 0$, and,

$$\sigma_{yield}(\zeta) = \sigma^0_{yield}\left(1-\frac{3}{2}\alpha\zeta^2\right) \tag{37}$$

III. Comparison with Experiments

The network yield stress depicted in Eq. (37) can be readily compared to the experimental yield stress of concentrated, strongly flocculated suspensions measured by Leong *et al.*[16] and Avramidis and Turian[17] using a vane-tool method. The prediction that the network yield stress decreases linearly with the square of the zeta potential agrees very well with the experimental observations.[16,17]

Experiments on flocculated suspensions generally have shown that σ_{yield} increases as a power law with respect to particle concentration with the exponent m ranging from 3 to 5. Using Eqs. (28) and (29), this implies a fractal dimension $1.75 < D < 2.2$, which agrees with the fractal dimensions of colloidal aggregates commonly found under fast-aggregation conditions[43–46] or slow-aggregation conditions.[23,24,47–49]

For all ζ, σ_{yield} follows a $(1/R^{d-3/2})$ dependence. With $d = 3$, Eqs. (35) and (36) predict that σ_{yield} decreases as a power law of particle size; i.e., $\sigma_{yield} \propto a^{-3/2}$, where $a = 2R$ is the particle size. In most experiments, σ_{yield} has been fitted to a power law of a^{-2}. In the experiments of Leong *et al.*,[15] $\sigma_{y,max} \propto a^{-2.05}$ has been obtained from the slope of the log–log plot of $\sigma_{y,max}/\phi^4$ versus a, where $\sigma_{y,max}$ is the maximum shear yield stress at the IEP. However, the data are quite scattered, and the slope has a range from −1.2 to −4.2.[15] The present exponent, −3/2, falls within this range. In the experiments of Buscall and co-workers[18,20] on polystyrene spheres, $\sigma_y \propto a^{-2}$ has been established by collapsing $\sigma_y a^2$ versus ϕ onto one curve, where σ_y is the shear yield stress. To compare with the $a^{-3/2}$ dependence predicted by the present theory, we have replotted the data of Buscall and co-workers[18,20] as $\sigma_y a^{3/2}$ versus ϕ in Fig. 10. For all particle sizes, $\sigma_y a^{3/2}$ versus ϕ collapses onto one power-law curve, indicating that the shear yield stress can be well fitted to an $a^{-3/2}$ dependence. Meanwhile, in their consolidation studies of zirconia and alumina, Miller *et al.*[50] also have analyzed the particle-size dependence of their compressive yield stress P_y by plotting $P_y a^2$ versus ϕ. They have shown that $P_y a^2$ versus ϕ falls on one curve for both zirconia and alumina but that $P_y a^2$ versus ϕ does not follow a power-law or exponential dependence on ϕ. P_y should be closely related to σ_y. To compare the compressive yield stress with the present $a^{-3/2}$ dependence, we have replotted the data from Ref. 50 as $P_y a^{3/2}$ versus ϕ in Fig. 11. Also shown in Fig. 11 are the data points for alumina taken from Refs. 5 and 51. For both zirconia and alumina of various sizes, $P_y a^{3/2}$ versus ϕ also falls on one curve, indicating that P_y can be fitted with an $a^{-3/2}$ dependence as well.

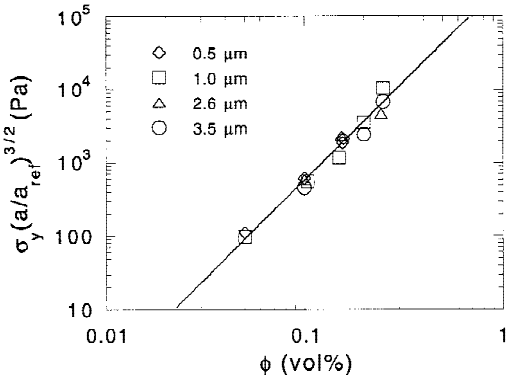

Fig. 10. $\sigma_y(a/a_{ref})^{3/2}$ versus volume fraction of flocculated polystyrene suspensions, where σ_y is the shear yield stress, and a and a_{ref} the particle diameter and the reference particle diameter, respectively. Data were taken from Refs. 18 and 20. That all the data points collapse on a single line indicates that σ_y can be well fitted to the $\alpha^{-3/2}$ power-law dependence, as predicted by the present theory.

Equation (36) predicts for $\zeta = 0$ that σ_{yield} decreases as a power law of the adsorbed-layer thickness with an exponent of −3/2. A quantitative comparison of Eq. (36) can be made with the recent experiments of Leong *et al.*[16] on zirconia particles adsorbed with different adsorbing species,[16] which show that the maximum σ_{yield} at the IEP decreases as the length of the adsorbing species increases. The lowering of the maximum σ_{yield} at $\zeta = 0$ by the adsorbed layer cannot be accounted for by the change in the Hamaker constant because of the adsorbed layer alone, i.e., the void[52] effect.[16] Furthermore, Leong *et al.*[16] have suggested that the finite maximum σ_{yield} without added adsorbing species is due to an adsorbed water layer on the particle surface. Assuming that there is an adsorbed water layer between the added adsorbed molecules and the particle surface and that the added adsorbed-layer thickness is the average of the maximum and minimum lengths of the adsorbing molecules,[16] designated d_{ave}, the closest surface-to-surface interparticle distance then is $s_0 = 2(d_{ave} + d)$, where d is the width of the possible adsorbed water layer. We have plotted σ_{yield} versus s_0 in Fig. 12. σ_{yield} follows a $s_0^{-3/2}$ power law when d is fitted to be 3.0 Å, which agrees with the known size of a water molecule.[53,54] Meanwhile, using their numerical fitting algorithm, Leong *et al.*[16] obtained an exponent of 1.27 (which gives 2.35 Å for the water-layer thickness[16]), close to the present prediction for the exponent of −3/2 (which gives 3.0 Å for the water-layer thickness). The inverse of the exponent corresponds to the parameter n in Ref. 16. Thus, the −3/2 power-law dependence of σ_{yield} on the closest separation, s_0, predicted by Eq. (36), also seems quite reasonable.

The experiment of Buscall and co-workers[18,20] on flocculated latex suspensions has shown that the power law of σ_{yield} has the same exponent, $m \approx 4.0$, as that of the shear modulus with respect to particle concentration, supporting the present hypothesis that ϵ_{yield} is independent of the particle concentration. That ϵ_{yield} is independent of particle concentration is fur-

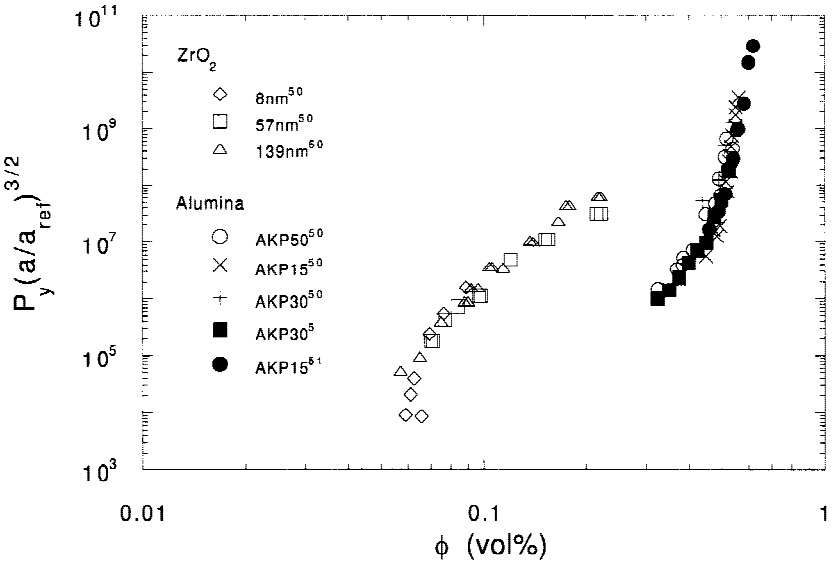

Fig. 11. $P_y(a/a_{ref})^{3/2}$ versus volume fraction of flocculated zirconia and alumina suspensions, where P_y is the compressive yield stress, and a and a_{ref} the particle diameter and the reference particle diameter, respectively. Data were taken from Refs. 5, 50, and 51. For both zirconia and alumina, all the data points collapse on a single line, indicating that P_y can be well fitted to the $a^{-3/2}$ power-law dependence, as predicted by the present theory.

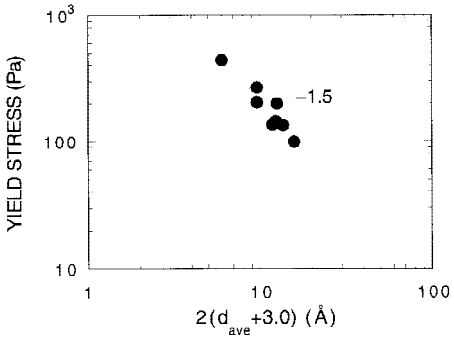

Fig. 12. Maximum shear yield stress versus s_0, where $s_0 = 2(d_{ave} + d)$, the maximum shear yield stress is the yield stress at the IEP, d_{ave} the average of the maximum and minimum conformation lengths of the adsorbed molecules taken from Ref. 16, and d the width of the water layer between the particle surface and the adsorbed molecules, as suggested by Ref. 16, with $d = 3.0$ Å, that agrees with the known molecular size of water. Least-squares fit gives a slope −1.5, in agreement with the present prediction.

ther supported by the direct measurements of ϵ_{yield} on the boehmite gels. Figure 13 shows ϵ_{yield} of the boehmite gels versus concentration taken from the experiments described in Ref. 23, where ϵ_{yield} is defined as the strain where G' and G'' cross. ϵ_{yield} fluctuates about a mean value of 13% as particle concentration increases, further supporting that ϵ_{yield} is independent of particle concentration.

Equations (31) and (32) can be used to estimate the yield strains for the boehmite gel and the alumina suspension shown in Figs. 2 and 3. The zeta potential for boehmite at pH 3.5 is ~60 mV (Ref. 27) and that for alumina at pH 8.5 is ~25 mV (Ref. 28). If we use Eq. (31) with $s_0 = 6.0$ Å, we obtain $\epsilon_{yield} = 12.6\%$ for the boehmite gels and 2.4% for the alumina suspension, which compare well with the experimental values, 13% for the boehmite gel and 0.5% for the alumina suspension, as shown in Figs. 13 and 3, respectively. Meanwhile, in recent experiments of Cannell and Zukoski[55] on flocculated alumina (AKP-15, Alcoa, Pittsburgh, PA) suspensions, $\epsilon_{yield} = 0.3\%$ has been obtained at pH 9 for the lowest concentration, where the suspension continues to exhibit a linear viscoelastic behavior at small strains. At pH 9, the zeta potential of alumina is approximately zero. Using Eq. (32) with $s_0 = 6.0$ Å and $2R = 1.3$ μm, we obtain $\epsilon_{yield} = 1\%$ for the AKP-15 suspensions at pH 9, which also compares reasonably with the experimental value of 0.3%.

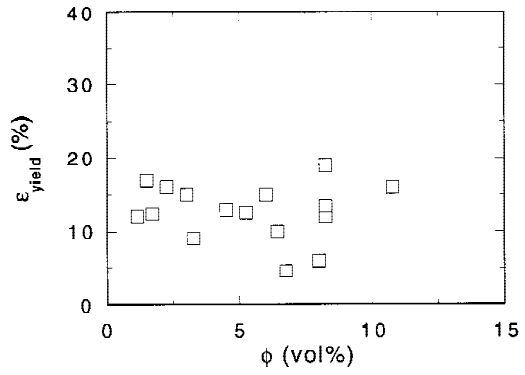

Fig. 13. Yield strain versus concentration for boehmite gels where the yield strain is defined as the strain amplitude at which G' and G'' cross. See Ref. 23 for the experimental details of the boehmite gels.

IV. Discussion

It is worth differentiating the suspension yield strain discussed in this paper from the limit of linearity that has been studied.[23,24,30] The limit of linearity is termed critical strain in Ref. 30. In a strain-controlled rheology test, the limit of linearity marks the onset of nonlinearity in the solid regime above which G' starts to deviate from a constant value while the yield strain marks the onset of the solid-to-liquid transition at which G' and G'' cross. In a vane-tool strain-rate-controlled experiment, the strain being proportional to time, the solidlike phase corresponds to a regime where the measured stress increases linearly with time. In a vane-tool experiment, the limit of linearity would manifest itself as a characteristic time beyond which the measured stress no longer increases linearly with time and the yield strain at another characteristic time beyond which the measured suspension stress becomes more-or-less independent of time. In the strain-controlled experiments, $G'' \propto \epsilon^{-1}$ when the suspension is well in the liquid regime.[56,57] Because $G'' >> G'$ in the liquid regime, the ϵ^{-1} dependence of G'' implies a constant stress in the liquid regime. Thus, the notion that yielding occurs when the suspension stress becomes constant from a vane-tool experiment is consistent with the present criterion that yielding occurs as the suspension undergoes a solid-to-liquid transition.

Extensive breakage of the bonds is required for the suspension to flow. Yielding should occur when the suspension strain approaches the two-particle yield strain. Hence, the suspension yield strain is not very sensitive to the change in particle concentration. Unlike the yield strain, the limit of linearity involves far less breakage of the bonds. How the first few bonds break depends on the structure of the network.[23,24] Thus, unlike the yield stain, the limit of linearity exhibits a concentration dependence. It generally decreases with an increasing particle concentration.[23,24,30] Although the limit of linearity may vary with concentration, it should not exceed the two-particle yield strain. Therefore, the highest limit of linearity measured at low concentrations should approach the two-particle yield strain and be about the same as the suspension yield strain. Indeed, in the boehmite gels, the highest limit of linearity was measured at ~12%,[23,24] very close to the mean value of the yield strain, 13%, shown in Fig. 13.

Many researchers have deduced the suspension yield stress

and yield strain in terms of the radial (tensile) two-particle yield strain by considering a short-range repulsion[33] or an exponentially decaying potential.[32] We consider a short-range repulsion, such as the one provided by an adsorbed layer, to find out if a short-range repulsion or an exponentially decaying potential alter our conclusion for the elastic and yield behavior. The short-range repulsion typically provides a very small elastic region in the radial direction. In the analysis of de Rooij *et al.*,[33] the two-particle yield strain, C_f, has been deduced by taking the interparticle interaction as the sum of the van der Waals attraction and the steric repulsion due to the adsorbed layer. They have deduced an equilibrium interparticle separation at $h_c = 7.82$ nm and an inflection point at $h_{cl} = 7.85$ nm when the adsorbed layer thickness is 3.85 nm. C_f can be estimated as $(h_{cl} - h_c)/(2R + h_c) \propto 0.08\%$, which is negligibly small. Although the authors used another quantity $(h_{c2} - h_c)/(2R + h_c)$, where h_{c2} is the separation at which the interparticle interaction energy becomes $3k_BT/2$, to estimate C_f, the obtained $C_f \propto 1.3\%$ is too small to account for the observed high limit of linearity in this system.[33] As discussed above, the highest limit of linearity measured at low concentrations should be upper bounded by the two-particle yield strain. The experimental highest limit of linearity measured for this system is ~14%,[30] much larger than the $C_f \approx 1.3\%$ proposed by these authors. The value of h_c, is very close to twice the adsorbed-layer thickness. If one considers the lateral movements instead and approximates h_c as s_0, the two-particle lateral (shear) yield strain can be estimated by $(2/3)^{1/2}[h_c/(2R + h_c)]^{1/2}$, as depicted in Eq. (32), and the obtained two-particle yield strain is ~11%, more comparable to the experimental highest limit of linearity, 14%. Therefore, even with a short-range repulsion, the conclusion that the lateral movements between the particles dominate the elastic and yield behaviors of a flocculated suspension remains valid.

In general, there can be two minima with an exponentially decaying potential, such as the electrostatic repulsion energy depicted in Eq. (4). There is no inflection point associated with the primary minimum at $s = 0$. Therefore, as we have discussed in Section II, as long as the secondary minimum is absent, the consideration of an exponentially decaying potential does not alter our conclusion that the lateral movements dominate the elastic and yield behaviors of a strongly flocculated suspension. The yield strain and the yield stress decrease linearly with the square of the zeta potential, with a finite zeta potential. There is ample evidence for the yield stress in the existing experiments.[16,17] If the ionic concentration is not high enough and/or the surface potential is not low enough, the interparticle interaction energy may have a secondary minimum. There can be two inflection points for radial movements around the secondary minimum, one for elongation and one for compression. The radial movements indeed can be elastic around the secondary minimum. However, the movements in the lateral direction continue to provide a lower two-particle yield force than in the radial direction. It can be readily shown from Eqs. (9) and (19) that $F_y \approx F_x y/r_0$. The yield force in the lateral directions is slightly less than that in the radial direction by a factor y/r_0. Thus, the lateral movements continue to be important even when the secondary minimum of the DLVO potential is present. The presence of a secondary minimum in the DLVO potential would not only greatly reduce the yield stress but also greatly increase the yield strain. We will examine, in a future publication, the yield strain and yield stress of weakly flocculated suspensions, where the influence of the secondary minimum is important. Meanwhile, the prediction that the yield strain decreases with an increasing zeta potential, as shown in Eq. (31), is valid only when the electrolyte concentration is low and s_0 is small. At higher electrolyte concentrations or larger s_0, the yield strain may behave differently. For example, in Ref. 55, the yield strains of flocculated alumina suspensions with 1*M* ammonium cloride have been shown to increase with an increasing zeta potential. In a future publication, we also will extend the examination to high electrolyte concentrations and large s_0.

V. Conclusions

We have theoretically examined the yield behavior of strongly flocculated suspensions based on the DLVO interactions. The DLVO interactions lack an inflection point under strongly attractive conditions, i.e., in the absence of a secondary minimum. As a result, there is no elastic response if the force is applied along the center-to-center direction between two particles. Hence, the radial movements, although commonly thought of as the yield mechanism of a network,[16] cannot account for the elastic behavior exhibited by colloidal gels. On the other hand, when the force is applied perpendicular to the center-to-center direction, particles can move elastically, and the yield force for such perpendicular motion is smaller than that of the radial motion by a factor of

$$\left(1 - \frac{1}{2}\alpha\zeta^2\right)\left(\frac{s_0}{r_0}\right)^{1/2}$$

as shown in Eq. (26). Because of the elastic response observed in colloidal gels and the ease of particles to move in the direction perpendicular to the center-to-center line, yielding of a network should be largely facilitated by lateral motions, which agrees with the shear melting experiment of colloidal crystals.[42]

Furthermore, we show that the lateral motion can remain elastic up to a distance

$$y_{max} \approx \left(\frac{2}{3}\right)^{1/2}\left(1 - \frac{1}{2}\alpha\zeta^2\right)(s_0 r_0)^{1/2}$$

beyond which yielding takes place. We approximate that the yielding of a particulate network occurs when the perpendicular displacements of all the bonds in a certain direction reach y_{max}. Thus, the yield strain is

$$\epsilon_{yield} = y_{max}/r_0 \propto \left(1 - \frac{1}{2}\alpha\zeta^2\right)\left(\frac{s_0}{r_0}\right)^{1/2}$$

The assumption that the yield strain is independent of particle concentration seems to agree with direct yield-strain measurements on boehmite gels, as shown in Fig. 13, as well as surfactant-coated alumina suspensions.[29] Furthermore, a concentration-independent yield strain implies that the yield stress should have the same exponent as the shear modulus as a power-law function of the concentration, which is in agreement with the experiments.[18,20]

The yield stress of a particulate network can be expressed as Eqs. (35) and (36) with the lateral yield force (Eqs. (14) and (23)) between individual particles as the yield force of the individual springs of a spring network and a previous theory for the elasticity of spring networks.[23] The prediction that yield stress decreases linearly with the square of the zeta potential has been observed in many experiments.[16,17] That the yield stress increases as a power law of particle concentration with the same exponent *m* as the shear modulus also agrees with experiments. Also, that the shear yield stress and the compressive yield stress P_y decrease as a power law of particle diameter with an exponent of −3/2 also agrees well with the results on polystyrene,[18,20] zirconia,[50] and alumina,[5,50,51] and it falls within the uncertainty of the experiments of Leong *et al.*[15] Finally, yield stress also decreases as a power law of the adsorbed layer thickness with an exponent of −3/2, which also is in good agreement with the experimental value of 1.27.[16]

Acknowledgment: This work was supported in part by the Army Research Office Multidisciplinary University Research Initiative (ARO/MURI)

(DAAH04-95-1-0102), the Air Force Office of Scientific Research (F49620-96-1-0191), and the National Science Foundation (DMR-9712773).

References

[1]I. A. Aksay, "Microstructure Control through Colloidal Consolidation"; pp. 94–104 in Advances in Ceramics, Vol. 9, *Forming of Ceramics.* Edited by J. A. Mangels and G. L. Messing. American Ceramic Society, Columbus, OH, 1984.

[2]F. F. Lange, "Powder Processing Science and Technology for Increased Reliability," *J. Am. Ceram. Soc.*, **72**, 3 (1989).

[3]W.-H. Shih, L. L.-L. Pwu, and A. A. Tseng, "Boehmite Coating as a Consolidation and Forming Aid in Aqueous Silicon Nitride Processing," *J. Am. Ceram. Soc.*, **78**, 1252 (1995).

[4]W.-H. Shih, D. J. Farrell, and W. Y. Shih, "Green-State Deformation of Boehmite-Coated Silicon Nitride Compacts"; pp. 233–40 in Ceramic Transactions, Vol. 62, *Science, Technology, and Commercialization of Powder Synthesis and Shape-Forming Processes.* Edited by J. J. Kingsley, C. H. Schilling, and J. H. Adair. American Ceramic Society, Westerville, OH, 1996.

[5]C. H. Schilling, "Plastic Shaping of Colloidal Ceramics"; Ph.D. Thesis. University of Washington, Seattle, WA, 1992.

[6]O. O. Omatete, M. A. Janney, and R. A. Strehlow, "Gelcasting—A New Ceramic Forming Process," *Am. Ceram. Soc. Bull.*, **70**, 1641 (1991).

[7]A. C. Young, O. O. Omatete, M. A. Janney, and P. A. Menchhofer, "Gelcasting of Alumina," *J. Am. Ceram. Soc.*, **74**, 612 (1991).

[8]A. J. Fanelli, R. D. Silvers, W. S. Frei, J. V. Burlew, and G. B. Marsh, "New Aqueous Injection Molding Process for Ceramic Powders," *J. Am. Ceram. Soc.*, **72**, 1833 (1989).

[9]T. K. Yin, I. A. Aksay, and B. E. Eichinger, "Lubricating Polymers for Powder Compacting"; pp. 654–62 in Ceramic Transactions, Vol. 1, *Ceramic Powder Science II.* Edited by G. L. Messing, E. R. Fuller Jr., and H. Hausner. American Ceramic Society, Westerville, OH, 1988.

[10]B. V. Velamakani, J. C. Chang, F. F. Lange, and D. F. Pearson, "New Method for Efficient Colloidal Particle Packing via Modulation of Repulsive Lubricating Hydration Forces," *Langmuir*, **6**, 1323 (1990).

[11]J. C. Chang, F. F. Lange, and D. S. Pearson, "Viscosity and Yield Stress of Alumina Slurries Containing Large Concentration of Electrolyte," *J. Am Ceram. Soc.*, **77**, 19 (1994).

[12]L. Bergström, C. H. Schilling, and I. A. Aksay, "Consolidation Behavior of Flocculated Alumina Suspensions," *J. Am. Ceram. Soc.*, **75**, 3305 (1992).

[13]W. Y. Shih, W.-H. Shih, S. I. Kim, and I. A. Aksay, "Equilibrium Density Profiles of Centrifuged Cakes," *J. Am. Ceram. Soc.*, **77**, 540 (1994).

[14]W. Y. Shih, W.-H. Shih, C. H. Schilling, and I. A. Aksay, "Density Profiles of Pressure-Filtered Cakes," unpublished work.

[15]Y.-K. Leong, P. J. Scales, T. W. Healy, and D. V. Boger, "Effect of Particle Size on Colloidal Zirconia Rheology at the Isoelectric Point," *J. Am. Ceram. Soc.*, **78**, 2209 (1995).

[16]Y. K. Leong, P. J. Scales, T. W. Healy, D. Boger, and R. Buscall, "Rheological Evidence of Adsorbate-Mediated Short-Range Steric Forces in Concentrated Dispersions," *J. Chem. Soc. Faraday Trans.*, **89**, 2473 (1993).

[17]K. S. Avramidis and R. M. Turian, "Yield Stress of Laterite Suspensions," *J. Colloid Interface Sci.*, **143**, 54 (1991).

[18]R. Buscall, I. J. McGowan, P. D. A. Mills, R. F. Stewart, D. Sutton, L. R. White, and G. E. Yates, "The Rheology of Strongly Flocculated Suspensions," *J. Non-Newtonian Fluid Mech.*, **24**, 183 (1987).

[19]D. G. Thomas, "III. Laminar-Flow Properties of Flocculated Suspensions," *AIChE J.*, **7**, 431 (1961).

[20]R. Buscall, P. D. Mills, J. W. Goodwin, and D. W. Lawson, "Scaling Behavior of the Rheology of Aggregate Networks Formed from Colloidal Particles," *J. Chem. Soc. Faraday Trans.*, **84**, 4249 (1988), and references therein.

[21]M. C. Grant and W. B. Russel, "Volume-Fraction Dependence of Elastic Moduli and Transition Temperatures for Colloidal Silica Gels," *Phys. Rev. E: Stat. Phys., Plasmas, Fluids, Relat. Interdiscip. Top.*, **47**, 2606 (1993).

[22]R. Buscall, I. J. McGowan, and C. A. Mumme-Young, "Rheology of Weakly Interacting Colloidal Particles at High Concentration," *Faraday Discuss. Chem. Soc.*, **90**, 115 (1990).

[23]W.-H. Shih, W. Y. Shih, S.-I. Kim, J. Liu, and I. A. Aksay, "Scaling Behavior of the Elastic Properties of Colloidal Gels," *Phys. Rev. A: Gen. Phys.*, **42**, 4772 (1990).

[24]W.-H. Shih, J. Liu, W. Y. Shih, S. I. Kim, M. Sarikaya, and I. A. Aksay, "Mechanical Properties of Colloidal Gels," *Mater. Res. Soc. Symp. Proc.*, **155**, 83 (1989).

[25]R. C. Sonntag and W. B. Russel, "Elastic Properties of Flocculated Networks," *J. Colloid Interface Sci.*, **116**, 485 (1987).

[26]C. J. Nederveen, "Dynamic Mechanical Behavior of Suspensions of Fat Particles in Oil," *J. Colloid Sci.*, **18**, 276 (1963).

[27]W.-H. Shih and L.-L. Pwu, "Rheology of Aqueous Boehmite-Coated Silicon Nitride Suspensions and Gels," *J. Mater. Res.*, **10**, 2808 (1995).

[28]S. I. Kim, "Structure–Property Relationships of Aqueous Ceramic Particulate Systems"; Ph.D. Thesis. University of Washington, Seattle, Washington, 1989.

[29]H.-L. Ker and I. A. Aksay, "Rheological Characterization of α-Alumina Slurries Adsorbed with Anionic/Nonionic Surfactant Mixtures," unpublished work.

[30]R. de Rooij, D. van den Ende, M. H. G. Duits, and J. Mellema, "Elasticity of Weakly Aggregated Polystyrene Latex Dispersions," *Phys. Rev. E: Stat. Phys, Plasmas, Fluids, Relat. Interdiscip. Top.*, **49**, 3038 (1994).

[31]R. J. Hunter and S. K. Nicol, "The Dependence of Plastic Flow Behavior of Clay Suspensions on Surface Properties," *J. Colloid Interface Sci.*, **28**, 250 (1968).

[32]B. A. Firth and R. J. Hunter, "Flow Properties of Coagulated Colloidal Suspensions III. The Elastic Floc Model," *J. Colloid Interface Sci.*, **57**, 266 (1976).

[33]R. de Rooij, A. A. Potanin, D. van den Ende, and J. Mellema, "Steady Shear Viscosity of Weakly Aggregated Polystyrene Latex Dispersions," *J. Chem. Phys.*, **99**, 9213 (1993).

[34]W.-H. Shih, S. I. Kim, W. Y. Shih, C. H. Schilling, and I. A. Aksay, "Consolidation of Colloidal Suspensions," *Mater. Res. Soc. Symp. Proc.*, **180**, 167 (1990).

[35]P. C. Hiemenz, *Principles of Colloid and Surface Chemistry*. Marcel Dekker, New York, 1986.

[36]D. Tabor and R. Winterton, "The Direct Measurement of Normal and Retarded van der Waals Forces," *Proc. R. Soc. London, A*, **312**, 435 (1969).

[37]B. V. Derjaguin, *Theory of Stability of Colloids and Thin Films.* Consultant Bureau, New York, 1989.

[38]D. R. Clarke, "On the Equilibrium Thickness of Intergranular Glass Phases in Ceramic Materials," *J. Am. Ceram. Soc.*, **70**, 15 (1987).

[39]B. J. Tarasevich, "Colloidal Interaction and Packing of Nanometer-Sized Particles; Application to Gel Processing"; M.S. Thesis. University of Washington, Seattle, Washington, 1990.

[40]J. E. Lennard-Jones, "Cohesion," *Proc. Phys. Soc. London*, **43**, 461 (1931).

[41]W. D. Brown and R. C. Ball, "Computer Simulation of Chemically Limited Aggregation," *J. Phys. A: Math. Gen.*, **18** [9] L517–L521 (1985).

[42]B. J. Ackerson and N. A. Clark, "Shear-Induced Melting," *Phys. Rev. Lett.*, **46**, 123 (1981).

[43]C. Aubert and D. S. Cannell, "Restructuring of Colloidal Silica Aggregates," *Phys. Rev. Lett.*, **56**, 738 (1986).

[44]D. A. Weitz and M. Olivera, "Fractal Structures Formed by Kinetic Aggregation of Aqueous Gold Colloids," *Phys. Rev. Lett.*, **52**, 1433 (1984).

[45]P. Dimon, S. K. Sinha, D. A. Weitz, C. R. Safinya, G. S. Smith, W. A. Varady, and H. M. Lindsay, "Structure of Aggregated Gold Colloids," *Phys. Rev. Lett.*, **57**, 595 (1986).

[46]C. Bolle, C. Cametti, P. Codastefano, and P. Tartaglia, "Kinetics of Salt-Induced Aggregation in Polystrene Lattices Studied by Quasi-Elastic Light Scattering," *Phys. Rev. A: Gen. Phys.*, **35**, 837 (1987).

[47]D. A. Weitz, J. S. Hwang, M. Y. Lin, and J. Sung, "Limits of the Fractal Dimension for Irreversible Kinetic Aggregation of Gold Colloids," *Phys. Rev. Lett.*, **54**, 1416 (1985).

[48]D. A. Schaefer, J. E. Martin, P. Wiltzius, and D. S. Cannell, "Fractal Geometry of Colloidal Aggregates," *Phys. Rev. Lett.*, **52**, 2371 (1984).

[49]J. C. Rarity and P. M. Pusey, "Light Scattering from Aggregating Systems: Static, Dynamic (QUELS), and Number Fluctuations"; p. 219 in *On Growth and Form.* Edited by H. E. Stanley and N. Ostrowsky. Nijhoff, Dordrecht, The Netherlands, 1986.

[50]K. T. Miller, R. M. Melant, and C. F. Zukoski, "Comparison of the Compressive Yield Response of Aggregated Suspensions: Pressure Filtration, Centrifugation, and Osmotic Consolidation," *J. Am. Ceram. Soc.*, **79**, 2545 (1996).

[51]F. F. Lange and K. T. Miller, "Pressure Filtration: Consolidation Kinetics and Mechanics," *Am. Ceram. Soc. Bull.*, **66**, 498 (1987).

[52]D. B. Hough and L. R. White, "The Calculation of Hamaker Constants from Lifshitz Theory with Applications to Wetting Phenomena," *Adv. Colloid Interface Sci.*, **14**, 3 (1980).

[53]A. H. Norton, M. D. Danford, and H. A. Levy, "X-ray Diffraction Study of Liquid Water in the Temperature Range 4°–200°C," *Discuss. Faraday Soc.*, **43**, 97 (1967).

[54]J. Israelachvili, *Intermolecular and Surface Forces*, 2nd ed. Academic Press, London, U.K., 1992.

[55]G. M. Cannell and C. F. Zukoski, "Shear and Compressive Rheology of Aggregated Alumina Suspensions," *AIChE J.*, **43**, 1700 (1997).

[56]J. Liu, "Structures and Properties of Colloidal Systems of Nanometer-Sized Particles (Viscoelastic Properties)"; Ph.D. Thesis. University of Washington, Seattle, Washington, 1990.

[57]J. Liu, W.-H. Shih, W. Y. Shih, M. Sarikaya, and I. A. Aksay, "Nonlinear Viscoelasticity and Restructuring in Colloidal Silica Gels," *MRS EA*, **25**, 43 (1990). □